Energy and Earth Science
Vol. 3, No. 1, 2020
www.scholink.org/ojs/index.php/ees
ISSN 2578-1359 (Print) ISSN 2578-1367 (Online)

Original Paper

Multi-Phase Manganese Mineralization in the Noamundi Synclinorium, East Indian Shield

D. Chakraborty[1*] & T. K. Baidya[2]

[1] Ex-CSIR Research Fellow, Department of Geological Sciences, Jadavpur University, Kolkata, India

[2] Professor (Retd.), Department of Geological Sciences, Jadavpur University, Kolkata, India

[*] D. Chakraborty, Ex-CSIR Research Fellow, Department of Geological Sciences, Jadavpur University, Kolkata, India

Received: April 9, 2020 Accepted: April 17, 2020 Online Published: May 7, 2020

doi:10.22158/ees.v3n1p26 URL: http://dx.doi.org/10.22158/ees.v3n1p26

Abstract

Manganese mineralization associated with phyllites in and around Joda, Odisha belongs to the Iron Ore Group of Noamundi basin and is a part of Jamda-Koira belt of East Indian Shield. The present study area comprises low to medium grade tectonites containing economic resources of both iron and manganese. Present study is concentrated on Manganese mineralization. Field study and petro-mineralogical observations reveal syngenetic character of manganese ores comprising lowT higher oxides viz. pyrolusite, cryptomelane, manganite as major Mn-minerals along with highT lower oxides viz. jacobsite, bixbyite, braunite and hausmannite as minor Mn-minerals. The Mn-ore bodies and associated phyllites have undergone multiple phases of deformation and metamorphism followed by hydrothermal and supergene processes. Four deformational phases have been deciphered during field study. Geochemical analyses of ores and phyllitic host rocks show high values of Al_2O_3, TiO_2, Ba, Co, Ni, Cr, Cu, Sc, V, As, Zn but depletion of Sr, Yb, Sm, Nb. Geochemical data infer ores to be a recycling product originally derived from a mafic crustal source of tholeiitic character. Age data obtained from Sm-Nd ratio of two rock samples are 3.46 Ga and 2.79 Ga. Present work provides a critical assessment on the multiphase mineralization of manganese ores.

Keywords

manganese, recycling, joda, noamundi, India

1. Introduction

The present study area, in and around Joda, comprises the Precambrian Iron Ore Group (IOG) of the Noamundi Basin, Odisha, a part of the Mesoarchean greenstone belt (3.5-3.0 Ga) viz. Jamda-Koira belt of the East Indian Shield (EIS). Low to medium grade tectonites containing economic resources of both iron and manganese are themajor rock types of the regional Noamundi synclinorium. Manganese ores, in this area (lat: 21°46' - 22°10'N; long: 85°06' - 85°35' E) are hosted mainly by tuffaceous phyllites of the IOG (3.3-3.1 Ga, Saha et al.1988) in the eastern limb of the Noamundi synclinorium, whereas iron ores are associated with mainly quartzites and phyllites in some places. The principal mineralized areas of manganese are Bichakundi, Bamebari, Khondband, Guruda and Joribar in and around Joda.

Archean manganese and iron mineralization in greenstone belts are reported from limited occurrences viz. the Rio das Velhas deposit of Brazil (Machado & Carnerio, 1992; Teixeira et al., 1996; Martin et al., 1997), the Barberton greenstone belt of South Africa (De Wit et al., 1980; Anhaeusser & Wilson, 1981), the Yilgarn and Pilbara blocks of Western Australia (Condie, 1981; Hallberg & Glikson, 1981), the Sebakwian-Bulawayan-Shamvaian belt of Zimbabwe (Myers & Kröner, 1994; Windly, 1982), the Superior and Slave provinces of Abitibi belt, Canada (Goodwin, 1973; Dimroth et al., 1982), the Isua Formation of Greenland (Gross, 1986; Schidlowski, 1988), the Bababudan and Chitradurga belt of South India (Ramakrishnan et al., 1976; Chadwick et al., 1981a, b) and the Iron Ore Group (IOG) of the East Indian Shield (Roy, 1981; Saha, 1994, Ghosh, et al., 2015a, b). The greenstone rocks of the present area belong to the IOG, which overlies the Singhbhum Granite Type-A and underlies the Singhbhum Granite Type-B (Saha et al., 1988).

From the field study, it is observed that the manganese ore bodies exhibit their conformable character with the host phyllites which are often laminated and compositionally banded. Manganese ore bodies are mainly of four different types viz. massive, banded, colloform (pisolitic/botryoidal/reniform) and brecciated. From petrographic studies, it is revealed that manganese ore is characterized by minerals of low temperature higher oxides such as pyrolusite, cryptomelane, manganite as well as high temperature lower oxides such as braunite, bixbyite, jacobsite, hausmannite. The present area bears evidence of regional metamorphism from upper green schist facies to lower amphibolite facies with four phases of tectonic deformation. Basedupon analytical data of major, minor, trace and rare earth elements, enrichment of Al_2O_3, TiO_2, Cr, Sc, V, Ba, Co etc. is observed in both manganese ores and associated host rocks along with positive correlation between alumina-titania and alumina-magnesia.

Manganese and iron mineralization in and around Joda, Kendujhar district, Odisha, have been studied by Jones (1934), Dunn and Dey (1942), Roy (1968), Banerji (1977), Chakraborty and Majumdar (1986), Ghosh et al. (2015) covering different ore geological aspects. Despite the aforesaid work, there is ample scope for the work on Mn-mineralogy, geochemistry, geochronology and ore genesis which the present paper tries to incorporate. Manganese mineralization in the Joda-Noamundi sector reveals recycling of manganese through different phases of tectonic deformation and metamorphism followed by later hydrothermal and supergene processes.

2. Regional Geology and Stratigraphy

The East Indian Shield (EIS) (21°25°N lat. and 85°-88°E long) comprises two Precambrian cratonic blocks viz. the northern high grade metamorphic Chhotanagpur Granulite gneiss terrain and the southern low grade metamorphic Singhbhum Granite greenstone terrain, which are separated by the Singhbhum Orogenic Belt containing Dalma lavas and Singhbhum Group of rocks. Figure 1 shows the geological map of the EIS. The Singhbhum granite greenstone terrain is bounded by Singhbhum shear zone (200 km long) in the north and separated from the Proterozoic Eastern Ghat Mobile Belt by Sukinda thrust in the south. The generalized Stratigraphic succession in this Singhbhum craton after Saha et al. (1988) is given in Table 1.

The Singhbhum cratonic block comprises two Archean greenstone belts viz. Jamda-Koira belt along with Noamundi basin on the west and Gorumahisani-Badampahar-Daitari belt on the east. The Joda area with Mn-mineralized zones belongs to the Jamda-Koira belt and located in the eastern limb of the Noamundi synclinorium. Both manganese and iron ores are closely associated with Banded Iron Formation (BIF), metamorphosed volcanic and sedimentary rocks of the IOG. The basement rock of the IOG basin is dominantly Singhbhum Granite (Type-A). The Mesoarchaean succession in the Singhbhum crustal province begins with the Iron Ore Group (IOG), characterized by Banded Iron Formations (BIF), clastic sedimentary rocks and minor carbonates (Chakraborty & Majumder, 1986; Saha, 1994; Bhattacharya et al., 2007; Mukhopadhyay et al., 2008). IOG rocks are low grade metamorphosed and intruded by younger Singhbhum Granite (Type-B). Bonai-Keonjhar iron-manganese belt (Lat: 21°40’ and 22°15’ Nand Long: 85°00’ and 85°35’ E) in the IOG forms a 60 km long & 25 km wide synclinorium (Noamundi synclinorium), referred to as “Iron-Ore horse shoe” plunging variously to north and north east. The corresponding anticlinal core in the western part of the Noamundi synclinoriumis mainly occupied by the 3.3 Ga Bonai granite (Saha, 1994). BIF, which is an important volcano-sedimentary rock formation of the Archean Greenstone belt, broadly defines the outline of the synclinorium, are almost continuously exposed along the margin, while manganese ore bearing shales occur within the core region of the fold. The entire region displays the effect of superposed folding on two near perpendicular axes, the generalised trends being NNE-SSW & WNW-ESE to NW-SE (GSI report on manganese ore, 2011). Mn-mineralization in and around Joda has taken place in Joda, Bichakundi, Khondband, Guruda, Joribar and Bamebari areas.

3. Previous Work

Manganese mineralization in the Noamundi-Jamda-Koira belt is a very conspicuous feature in close association with iron ores. Spencer (1948) considers manganese ores hydrothermal in origin but Sen (1951) regards them to be submarine volcanic origin. Engineer (1956), Prasad Rao and Murty (1956) consider the manganese ores products of the replacement of shales and quartzites by manganiferous solutions. Basu (1969) considers these ores syngenetic but modified by epigenetic concentration. Basu (1969) and Roy (1978) describe bedded manganese orebodies interstratified with shale (often

tuffaceous) and sometimes co-folded with it from Kalimati, Phagua, Gurda Block II and the Mahulsukha mine-areas in Odisha (cf. Roy, 1981). Murthy and Ghosh (1971) reported pyrolusite-cryptomelane-manganite-rhodochrosite bearing Mn-ores in association with chert and dolomite beds and regarded the manganese minerals originally disseminated in the shales and later mobilized and concentrated at structurally favourable sites. Banerji (1977) concluded that manganese ores formed later than the iron ores. Subramanyam and Murty (1975) and Banerji (1977) suggest a volcanic source for the manganese deposits. Banerji (1977) stratigraphically characterized iron-manganese mineralization in the Jamda-Koira belt as the Noamundi Group of much younger age (c.1500-1100 Ma) with the following sequence (ascending order) lower shale (tuffaceous shale–phyllite), banded hematite jasper, upper shale (manganiferous shale, tuff and chert), basic intrusion, grinitic activity. Sarkar and Saha (1962, 1977) described manganese ore bodies intimately associated with unmetamorphosed shales (occasionally tuffaceous) and chert of the Archean IOG. According to Roy (1981), Mn-oxide deposits are intimately associated with unmetamorphosed shales (occasionally tuffaceous) and cherts of the Precambrian IOG rocks and the manganese ores are of dominantly lateritoid type having mainly pyrolusite and cryptomelane with local manganite. There are a number of manganese ore bodies within chert and/or shale as layers and lenses (Banerji, 1977; Mohapatra et al., 1996; Mishra et al., 2006). Mishra et al. (2006) classified the IOG manganese orebodies into stratiform, stratabound, and lateritic types. The stratiform type has distinct lamination or banding, and is often co-folded with shale. The stratabound type is structure- and shear zone-controlled and is often silicified. These ore bodies occasionally cross-cut the bedding planes of the host shale.

4. Methodology

Samples of various types of ore and associated host rocks are collected from the open-pit mines and surrounding areas for geochemical analyses and isotopic studies. Petro-mineralogical work includes study under transmitted and reflected light microscopes, X-Ray Diffraction (XRD) study, Scanning Electron Microscopy (SEM), Energy Dispersive X-Ray (EDX) and Electron Probe Micro Analyzer (EPMA). SEM–EDX analysis of polished ore thin sections is done using INCA X-SIGHT software under accelerating voltage 20 kV and probe diameter 2 μm. EPM analysis is done using PIXITE software with an accelerating voltage of 15 kV, current of 12 nA and beam size of 1 μm. Major element, trace element and REE analyses of the ores and associated rocks are done by the Australian Laboratory Services, Queensland with a combination of XRF and ICP-MS techniques after comminution of the samples to -300 mesh in contamination-free pulverizer. For the purpose of Sm/Nd isotopic study, two crushed rock samples are analyzed for their Sm and Nd abundances by isotopic dilution, and the isotopic composition of Nd by mass spectrometry. The isotopic composition of Nd is determined in static mode by Multi-Collector ICP-Mass Spectrometry. All isotope ratios are normalized for variable mass fractionation to a value of $^{146}Nd/^{144}Nd=0.7219$ using the exponential fractionation law. Sm isotopic abundances are measured in static mode by Multi-Collector ICP- Mass Spectrometry, and are normalized

for variable mass fractionation to a value of 1.17537 for $^{152}Sm/^{154}Sm$ also using the exponential law. Sm/Nd isotopic studies are done by ICP-SFMS at the Canadian laboratory of the Australian Laboratory Services.

5. Mode of Occurrence and Structural Disposition of Manganese Ores

Manganese ores occur as massive, thinly laminated or lenticular stratabound bodies hosted by differently coloured (red, pink, yellow, brown, purple, smoky grey, etc.) phyllites which are kaolinised in many parts to different degrees. Large deposits of manganese ores are being mined in Bichakundi (near Joda), Khondband, Bamebari, Guruda and Joribar areas in the eastern part of the Noamundi synclinorium. In Khondband and Guruda areas manganese ore bodies are very closely associated with iron ores. The massive Mn-ore bodies show typical colloform structures (often pisolitic and botryoidal). The ore bodies, in places, are co-folded with phyllites forming mesoscopic synforms and antiforms.

In the Joda area, manganese ore bodies are mainly hosted by phyllitic rocks with minor quartzites. The lenticular bands of manganese ore are conformable with the host phyllites. The phyllites are, in places, laminated, compositionally banded and often showing brecciated character (**Figure 2a**). The laminated phyllites are light coloured and mainly composed of very fine-grained phyllosilicates with intermittent occurrence of ferruginous chert. The geological field work reveals manganese ore bodies to be of four different types viz. massive, banded, colloform (pisolitic/botryoidal/reniform) and brecciated. In the quarry section, manganese rich ore pockets are overlain by ochre which in turn is capped by lateritic horizon (**Figure 2b**). At places, a high degree of strain has produced folds with rootless intrafolial character (**Figure 2c**). The associated iron ore bands comprise mainly hematite or martite with variable amounts of goethite and minor amounts of magnetite and siderite. Hematite-rich iron ores often show typical BIF character accompanied by strong deformational events (**Figure 2d**). The gangue material is principally composed of cherty silica (in the form of jasper or quartzite) and kaolinitic clay.

The manganese ores and associated host rocks bear the evidence of multiphase tectonic deformation. The F_1 and F_2 folds are more or less isoclinal and axial plane dipping towards NW or SE. The F_3 fold is transverse and superposed over F_1 and F_2 and is much more open in character with axial plane E-W in general. The major Mn-ore bodies are mainly localized in the axial zones of the F_2 folds (**Figure 2e**), thin manganese ore bands are concentrated along the S_2 axial plane (**Figure 2f**). The F_2 fold axis plunges 7^0 to 40^0 towards the NNE or the SW with local variations towards the NNW, E and ENE. Manganese ore bands are also co-folded with the host phyllite forming mesoscopic synformal and antiformal structures (**Figure 2g & 2h**). The F_2 fold of the ore bodies can be categorized in Class 2 of Ramsay's geometrical classification of folds (Ramsay, 1967). The third phase of tectonic deformation (D_3), having a transverse compressive stress direction in comparison with D_1 and D_2, produced open type of cross folds (F_3) (**Figure2i**) which in turn resulted in small dome and basin structures with axial culmination and depression. This corresponds to Type-I interference pattern of Ramsay (1967). Rootless intrafolial fold of D_1/F_1 generation is also observed in the field (**Figure2c**). The axis of F_3 plunges 10^0 to 62^0 towards

WNW mainly with variations of W, NW and SE. The D_3 phase was further followed by a phase of faulting and shearing (D_4) (**Figure 2j**) which formed a number of sets of faults in this region among which at least three sets of faults are discernible in the field, the attitudes of which are as follows:

i) 60^0 to 85^0 dipping towards W to NW.

ii) 8^0 to 10^0 dipping towards SE to NE.

iii) 60^0 to 65^0 dipping towards the SW.

The fault and shear zones are mostly in filled with pyrolusite-cryptomelane-chert association and fault breccias (**Figure 2k**). Although the Mn ores are not uncommon along the S_0 and S_1 planes, the ores are primarily concentrated in the F_2 hinge areas. Thinning of the ore bands at the limbs and thickening of the same at the hinge are very frequent in the manganese ore mineralized zone. The folded ore bodies have two general axial trends NE to ENE and SW to WSW. The axial planes of these folded ore bodies dip between 40^0 and 72^0 towards NW or SE. In these areas, the ore bodies also plunge along the F_2 fold axis (**Figure2l**).

6. Mineralogy and Petrography of Manganese Ores

Study under microscopes (both reflected and transmitted light) reveals that the predominant manganese ore minerals are pyrolusite, cryptomelane and manganite. Braunite, bixbyite, jacobsite and hausmannite occur mainly as minor phases. Minor iron ore minerals like hematite/martite and goethite are also present. The associated gangue minerals include quartz, muscovite, biotite, kaolinite and glauconite.

Two generations of axial plane cleavage have been identified in the manganese ore. The first-generation cleavage (S_1) is conformable with the compositional banding/bedding (S_0) whereas the second-generation cleavage shows transgressive relation with S_0 and S_1 planes Manganese ore gets mainly concentrated along the F_2 hinge area (**Figure 3a**). The micro-folded veins of pyrolusite forming F_2 puckers exhibit their syn-kinematic character to D_2 phase of tectonic deformation (**Figure 3b**). Bixbyite crystals showing brecciated character are mostly fragmented at the edges with matching boundaries. As a secondary mineral, pyrolusite partly replaces bixbyite and the edges of the bixbyite crystals are rounded up in a few places (**Figure 3c**). Jacobsite grain is found as scattered within the silicate rich groundmass (**Figure 3d**). Well-developed braunite crystal is exhibiting its resorbed grain boundary replaced by polianite crystals of later generation (**Figure 3e**). Bands of colloform structure at the interstitial spaces of banded ore clasts are also present (**Figure 3f**) which contains altered braunite crystals of earlier generation. Second generation of pyrolusite rich vein is closely associated with hematite rich matrix (**Figure 3g**). Hematite-goethite rich vein was formed at a late stage which is little bit folded at places (**Figure 3h**). The possible weathering reactions deduced from textural studies are as follows:

2 Bixbyite+O_2=4 Pyrolusite/Polianite (Figure 3c)

4 Bixbyite+K^++$2O_2$+nH_2O=Cryptomelane (Figure 3c)

Braunite+$2O_2$=7 Pyrolusite+SiO_2 (Figure 3e)

7. Major Element Geochemistry

The average silica content in ores and associated phyllites (except 93% in one sample of Bamebari quartzite) are 9.07% and 45.68% respectively. The average alumina content in ores and phyllitic rocks are 7.49% and 26.65% respectively. The average TiO_2 content in phyllitic rocks is 2.96% with a maximum value up to 6.96%. The average MgO content is higher in phyllites (1.15%) than its average content in ore samples (0.22%). The average concentration of Fe_2O_3 in associated host rocks, manganese-bearing ores and iron ores are 7.4%, 14% and 59.7% respectively whereas the average concentration of MnO in host rocks, iron-bearing ores and manganese ores are 1.83%, 6.05% and >39% respectively. MnO shows an inverse relationship with almost all the major oxides except P_2O_5. Strong positive correlations among Al_2O_3, TiO_2, CaO are observed. The major element contents of manganese-iron ores, associated phyllites and quartzites are presented in **Table 2**.

8. Trace Element Geochemistry

41 trace elements are determined using ICP-MS techniques in some manganese ore samples and associated rocks of Joda. The data are presented in Table 3. It is observed that the average concentration of trace elements Cr, Co, Ni, Cu, Zn, As, Ba are 219ppm, 52.7ppm, 100.5ppm, 40.5ppm, 94.6ppm, 19.62ppm, 689.95ppm which are relatively higher in comparison to their average crustal abundances. It is also observed that there are strong positive correlations between Sc and Al_2O_3 (Figure 4a), V and Al_2O_3 (Figure 4b), Cr and Al_2O_3 (Figure 4c), Th and Al_2O_3 (Figure 4d), Ga and Al_2O_3 (Figure 4e), Nb and Al_2O_3 (Figure 4f). The average concentrations of Sc, V are found to be 11.6 ppm, 101.1 ppm respectively; there is a relative enrichment of Sc, V, Cr in comparison with average Zr & Th. The average Ba content varies from 205.6 ppm in host rocks to 1012.85 ppm in ores (maximum up to 2960 ppm) respectively. The average Pb content varies from 10 ppm in host rocks and 26.8 ppm in ores respectively. The average Cs content is 2.18 ppm and Cs is probably derived from psilomelane-rich ore. The average Rb content is 65 ppm, Rb generally replaces K and is always associated with potash bearing minerals. Chondrite normalized (after McDonough & Sun, 1995) Trace element pattern of manganese ores and associated rocks shows positive Co, As, Rb, Ba anomaly (Figure 7).

9. Rare Earth Element (REE) Geochemistry

The manganese ores and associated rocks of the Joda area are analyzed using Inductively Coupled Mass Spectrometry (ICP-MS) to determine the dispersion pattern of REE and their genetic implications. The REE concentration values are presented in Table 4. The La content ranges from 2 to 44.2 ppm. The average concentration of Ce is 25.71 ppm. The average contents of Pr (3.358 ppm), Sm (3.042 ppm), Eu (0.874 ppm) are low in comparison to other LREE. The average concentration of Nd is 13.2 ppm and it is observed that in all the samples under consideration, the concentration level of Nd is higher with respect to that of Pr, Gd and Dy are showing maximum concentration in comparison to other elements of HREE. The highest concentration of Gd is 5.9 ppm and highest concentration of Dy is 7.83 ppm. The total

content of HREE (146.67 ppm) is very low in comparison to the total LREE content (609.34 ppm). The average concentration of ΣHREE in all the samples is found to be 14.667 ppm in comparison to that of ΣLREE which is found to be 60.934 ppm**.**

All REE results have been normalized with North American Shale Composite (NASC, Haskin et al., 1968; **Figure 8a**) and also with average upper continental crust (Taylor & McLennan, 1981; **Figure 8b**). Both standard-normalized REE patterns exhibit similar trends. The diagrams depict an overall depletion of LREE and relative enrichment of HREE, an exception for an ore sample with diminished HREE value that can be attributed to preferential leaching of HREE by meteoric water in oxidized ores. The most significant feature of the REE pattern is the positive Eu anomaly of the ores and associated rocks. The average Eu/Eu* and Ce/Ce* values are 1.16 and 0.8 respectively.

In TiO_2-Zr/(P_2O_5 *10^4) discrimination diagram (**Figure 9**), there is a complete separation between the fields of tholeiitic and alkali basalts with alkali basalts plotting in the field of low Zr/ P_2O_5 and high TiO_2.

10. Sm-Nd Isotopic Studies and Age

Two rock samples are analyzed for Sm and Nd by isotope dilution. The details of the analytical results are given in Table 5. Model age for the Sm-Nd system is chosen for the purpose of present study as it can be calculated for an individual rock from a single pair of parent-daughter isotopic ratios. During model age calculations, one assumption is made about the isotopic composition of the reservoir from which the rock samples are ultimately derived. The age calculation of the two rock samples are carried out based on TDM (T-Depleted Mantle) model age as the initial $^{143}Nd/^{144}Nd$ ratios from Precambrian terrains suggest that the mantle which supplied the continental crust has evolved since earliest times with an Sm/Nd ratio greater than that of CHUR (Chondritic Uniform Reservoir). Moreover, fractionation of the rock samples is considered negligible after its separation from the mantle source.

Table 1. The Generalized Chrono Stratigraphic Succession of the Singbhum-Orissa Iron Ore Craton (after Saha et al., 1988)

Newer Dolerite dykes and sills		c. 1600-950 Ma	
Mayurbhanj Granite		c. 2100 Ma	
Gabbro-anorthosite ultramafics		c. 2100-2200 Ma	
Kolhan Group			
	Unconformity		
Jagannathpur Lava	Dhanjori-Simlipal lavas	(c. 2300 Ma)	
Malangtoli Lava	Quartzite-conglomerate		Dhanjori Group
Pelitic and arenaceous metasediments with mafic sills		(c. 2300-2400 Ma)	Singhbhum Group
	Unconformity		
Singhbhum Granite (Type B) (Phase III)		c. 3.1 Ga	
Mafic Lava, tuff, acid volcanics, tuffaceous shale			
Manganiferous shale and Mn-ores (Noamundi Group of Banerji, 1977),			Iron Ore Group
Banded hematite jasper, banded hematite quartzite with iron ores, Ferruginous chert, local dolomite and quartzite sandstone			
			Nilgiri Granite
Singhbhum Granite (Type A) (Phase I and II)		c. 3.3 Ga	
Folding and metamorphism of OMG and OMTG			Bonai Granite
Older Metamorphic Tonalitic Gneiss (OMTG)		c. 3.775 Ga	
Older Metamorphic Group (OMG): Pelitic schist, quartzite, para-amphibolite, ortho-amphibolite		c. 4.0 Ga	

Table 2. Major Element Oxide Contents of Manganese Ores and Associated Rocks in Joda Area, Odisha (in wt%)

Oxides	D1	D2	D3	D4	D5	D6	D7	D8	D9	D10	D11	D12	D13	D14	Fig Tree Shales[a]	Moodies Shales[b]	NASC[c]	ACPS[d]
SiO_2	60.05	53.07	55.35	30.07	92.8	3.63	5.7	0.71	7.7	3.55	57.96	27.44	20.24	12.16	60.49	59.32	64.82	66.9
Al_2O_3	17.64	13.72	17.3	12.7	0.27	0.64	3.42	1.14	6.12	2	22.02	43.72	45.51	26.44	11.86	13.93	17.5	16.67
Fe_2O_3	9.89	8.88	15.46	47.22	4.74	83	47.43	17.67	78.87	10.36	4.78	2.98	5.08	41.82	0.51	0.44	0.8	0.78
MgO	1.15	1.12	1.01	0.8	0.03	0.08	0.18	<0.01	0.05	0.26	1.12	2.19	0.31	0.22	8.56	7.36	5.7	5.87
CaO	0.07	0.1	0.06	0.04	0.03	0.04	0.18	0.09	0.02	0.31	6.06	8.36	8.28	6.07	0.11	0.13	0.25	0.06
Na_2O	<0.01	0.03	<0.01	0.01	<0.01	<0.01	0.02	0.01	<0.01	0.05	0.76	2.45	0.51	0.09	2.4	1.35	3.51	0.53
K_2O	3.72	3.84	3.59	3.78	0.06	0.02	1.11	0.35	0.08	2.13	0.43	1.89	0.38	0.68	5.82	5.1	2.83	2.59
MnO	0.16	11.1	0.03	0.21	1.06	1.36	27.2	>39	0.21	>39	0.03	0.04	0.43	1.27	2.45	4.87	3.97	4.97
TiO_2	1.48	1.35	1.4	1.82	0.02	0.03	0.22	0.03	0.53	0.05	1.79	4.81	6.96	4.09	1.04	1.76	1.13	1.5
P_2O_5	0.11	0.02	0.04	0.05	0.05	0.64	1.04	0.06	0.17	0.07	0.008	0.007	0.003	0.042	-	-	0.15	0.14
H_2O	-	-	-	-	-	-	-	-	-	-	4.63	5.22	10.07	6.67	-	-	-	-
LOI	5.11	5.24	5.07	2.92	0.35	10.75	12.08	11.04	6.62	12.53	4.84	5.76	12.2	6.96	6.69	5.75	-	-

Note. *D1-D quarry phyllite; D2-Bamebari phyllite; D3-H quarry phyllite, D4-Khondband iron ore; D5-Bamebari jasper quartzite; D6-H quarry manganese bearing iron ore; D7-Bamebari iron-manganese ore; D8-Khondband iron bearing manganese ore; D9-H quarry iron ore; D10-Khondband manganese ore; D11-Bamebari kaolinized phyllite; D12-H quarry kaolinized phyllite; D13-Guruda phyllite; D14-Khondband iron ore.

[a]Figtree Group (3.4 Ga) and [b]Moodies Group (3.3 Ga) of Swaziland Supergroup, S. Africa (McLennan & Taylor, 1983).

[c]North American Shale Composite (Gromet et al., 1984).

[d]Average Canadian Proterozoic (Aphebian) Shale (Cameron & Garrels, 1980).

Table 3. Trace Element Contents of Mn-Ores and Associated Rocks of Joda Area (in ppm)

Elements	D1	D2	D3	D4	D5	D6	D7	D8	D9	D10
Li	10	30	10	<10	10	<10	60	<10	<10	10
Sc	24	18	25	17	<1	4	9	2	10	6
V	254	121	291	93	6	28	52	12	122	32
Cr	430	200	600	300	10	140	60	10	420	20
Co	8	42	3	11	5	10	98	60	<1	289
Ni	64	160	55	14	19	183	294	27	39	150
Cu	28	57	45	5	10	16	132	14	19	79
Zn	18	93	21	15	13	163	289	56	39	239
Ga	22.5	11.7	23.7	21.2	1.6	3.9	8	6	8	7.5
Ge	5	<5	7	5	<5	<5	<5	<5	5	<5
As	5.3	5.1	3.6	4	8	5.2	133	6	18.4	7.6
Se	0.3	1	0.3	0.4	<0.2	0.6	1.9	0.6	0.5	1.7
Rb	142.5	88.8	138.5	163.5	2.2	0.8	32	7.4	3.2	71.9
Sr	7.4	39.8	10.4	7	5.3	2.9	112.5	206	1.5	384
Y	24.7	28	23.4	46	3.1	28.1	65	10.4	17.7	111.5
Zr	186	131	169	318	3	6	32	8	84	12
Nb	12.5	7.3	11.5	17.8	<0.2	0.4	1.9	0.5	5.1	0.5
Mo	<1	<1	<1	<1	1	<1	<1	<1	<1	<1
Pd	0.003	0.004	0.004	0.003	<0.001	<0.001	0.001	0.002	0.002	0.002
Ag	<0.5	0.5	<0.5	<0.5	<0.5	<0.5	1.7	2.7	<0.5	2.5
Cd	<0.5	<0.5	<0.5	<0.5	<0.5	<0.5	1	<0.5	<0.5	2
In	0.028	0.04	0.032	0.043	<0.005	0.012	0.028	0.007	0.03	0.022
Sn	4	2	4	5	<1	<1	1	<1	1	<1
Sb	0.17	0.05	0.18	0.63	0.05	0.34	0.12	0.21	0.18	0.18
Te	0.02	0.03	0.03	0.08	<0.01	0.04	0.06	0.06	0.05	0.02
Cs	3.75	3.47	3.81	2.48	0.08	<0.01	1.79	0.27	0.05	6.11
Ba	206	438	154.5	979	23.9	42.6	301	1670	124.5	2960
Hf	4.9	3.5	4.4	8.4	<0.2	0.2	0.8	0.2	2.3	0.3
Ta	1	0.6	1	1.6	<0.1	<0.1	0.1	<0.1	0.5	<0.1
W	1	<1	1	2	1	<1	<1	<1	1	2
Re	<0.001	<0.001	<0.001	0.001	<0.001	<0.001	0.001	0.002	0.001	0.002
Pt	0.0024	0.0038	0.003	0.0059	<0.0005	<0.0005	0.001	<0.0005	0.0017	<0.0005
Au	0.001	0.001	0.003	0.001	<0.001	0.001	0.001	0.004	0.001	0.005
Hg	0.005	0.044	0.017	0.059	<0.005	0.013	0.042	0.4	0.137	0.816

Tl	0.1	0.13	0.04	0.08	<0.02	<0.02	0.09	0.56	<0.02	0.58
Pb	6	18	14	17	<2	<2	21	56	10	55
Bi	0.13	0.08	0.07	1.48	0.01	0.02	0.05	0.04	0.06	0.08
Th	6.58	5.02	5.53	13.4	0.09	0.24	1.26	0.6	3.65	0.63
U	2.06	1.77	1.75	2.95	0.13	2.84	1.43	0.34	4.2	0.91

Table 4. ICP-MS Analytical Data for REEs in Mn-Ores and Associated Rocks of Joda Area (in ppm)

Elements	**D1**	**D2**	**D3**	**D4**	**D5**	**D6**	**D7**	**D8**	**D9**	**D10**
La	17.2	18.2	19.4	12	2	5.2	44.2	13.1	5.8	10.4
Ce	27.4	38.7	18.4	32.9	2.8	7.1	57	55.4	7.8	9.6
Pr	3.37	4.14	3.63	2.34	0.47	1.64	9.79	4.29	1.68	2.23
Nd	12.6	15.4	14.2	8.5	1.7	7.3	37.6	16.3	7.5	10.9
Sm	2.8	3.4	3.21	2.12	0.36	1.97	7.95	3.72	1.76	3.13
Eu	0.7	0.95	0.92	0.61	0.09	0.64	2.27	0.84	0.64	1.08
Gd	2.71	3.74	3.54	2.78	0.4	2.98	9	2.59	2.45	5.9
Tb	0.49	0.59	0.56	0.59	0.06	0.5	1.36	0.42	0.37	0.98
Dy	3.28	3.65	3.71	4.66	0.34	2.93	7.83	2.18	2.44	7.11
Ho	0.75	0.78	0.76	1.16	0.07	0.61	1.6	0.35	0.55	1.81
Er	2.43	2.29	2.33	4.17	0.19	1.68	4.33	0.84	1.75	5.99
Tm	0.37	0.35	0.35	0.71	0.03	0.23	0.56	0.11	0.29	0.79
Yb	2.47	2.22	2.34	5.35	0.17	1.44	3.38	0.7	1.87	4.46
Lu	0.38	0.36	0.37	0.85	0.02	0.24	0.54	0.09	0.29	0.76
ΣLREE	64.07	80.79	59.76	58.47	7.42	23.85	158.81	93.65	25.18	37.34
ΣHREE	12.88	13.98	13.96	20.27	1.28	10.61	28.6	7.28	10.01	27.8
ΣREE	76.95	94.77	73.72	78.74	8.7	34.46	187.41	100.93	35.19	65.14

Table 5. Sm-Nd Isotopic Data of the Host Rocks Associated with Mn-Ores in Joda Area

Sample Description	Sm (ppm)	Nd (ppm)	$^{147}Sm/^{144}Nd$	$^{143}Nd/^{144}Nd$	± 2 SE	TDM age (Ga)	ε_{Nd}^{0}
1. (Laminated phyllite, Bichakundi H-quarry)	2.944	12.73	0.1399	0.511805	0.000012	2.79	-16.3
2. (Associated BIF, Khondband mine)	1.913	7.951	0.1455	0.511603	0.000012	3.46	-20.2

Note. 1) Uncertainty in Nd isotopic composition is 2 Standard Errors; 2) TDM is the Depleted Mantle Model Age in Ga calculated using the linear model of Goldstein et al. (1984); 3) ε_{Nd}^{0} is the epsilon ^{143}Nd value calculated present day.

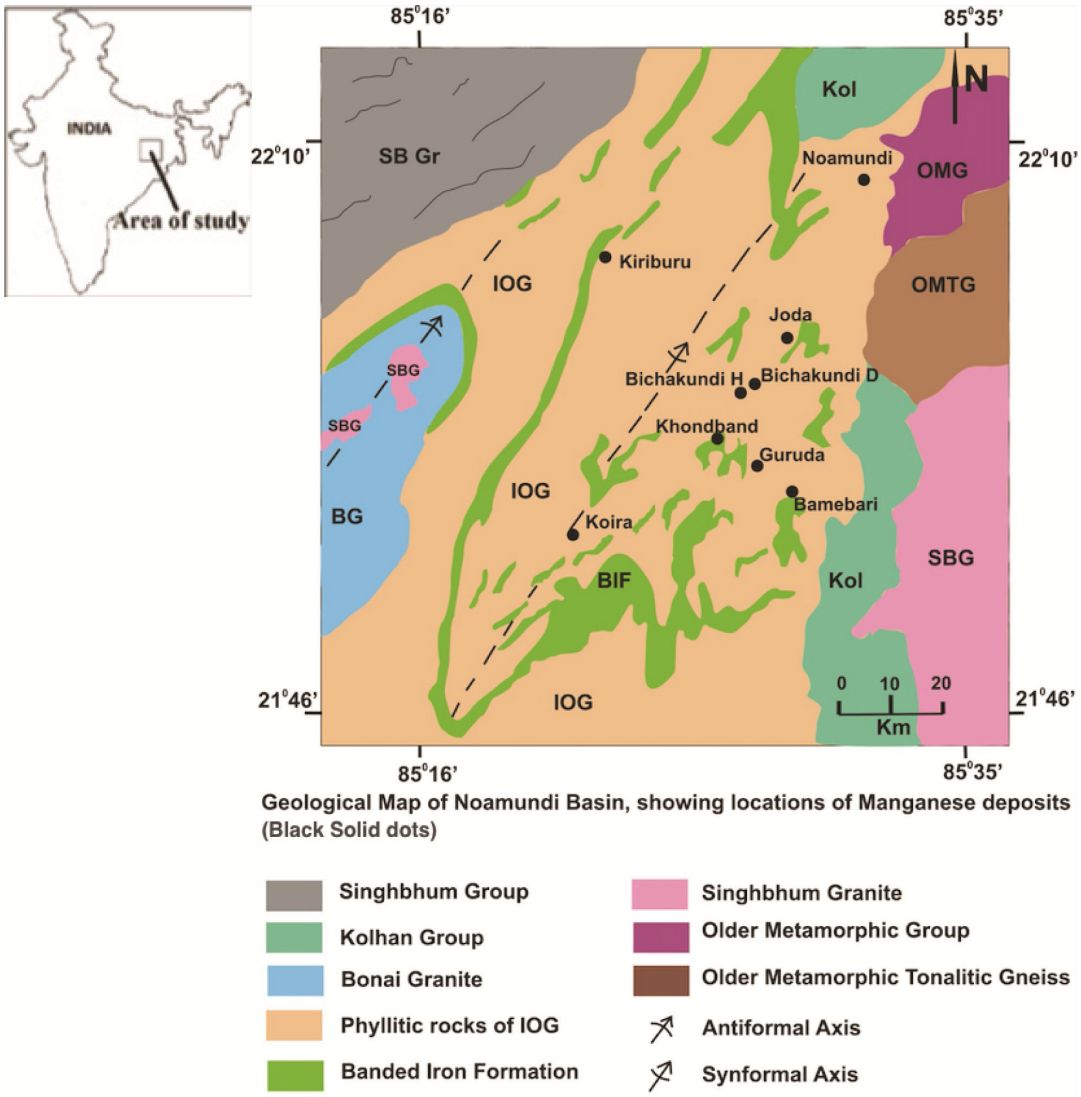

Figure 1. Geological Map of Noamundi Basin Showing Major Manganese Deposits In and Around Joda, Associated with BIF

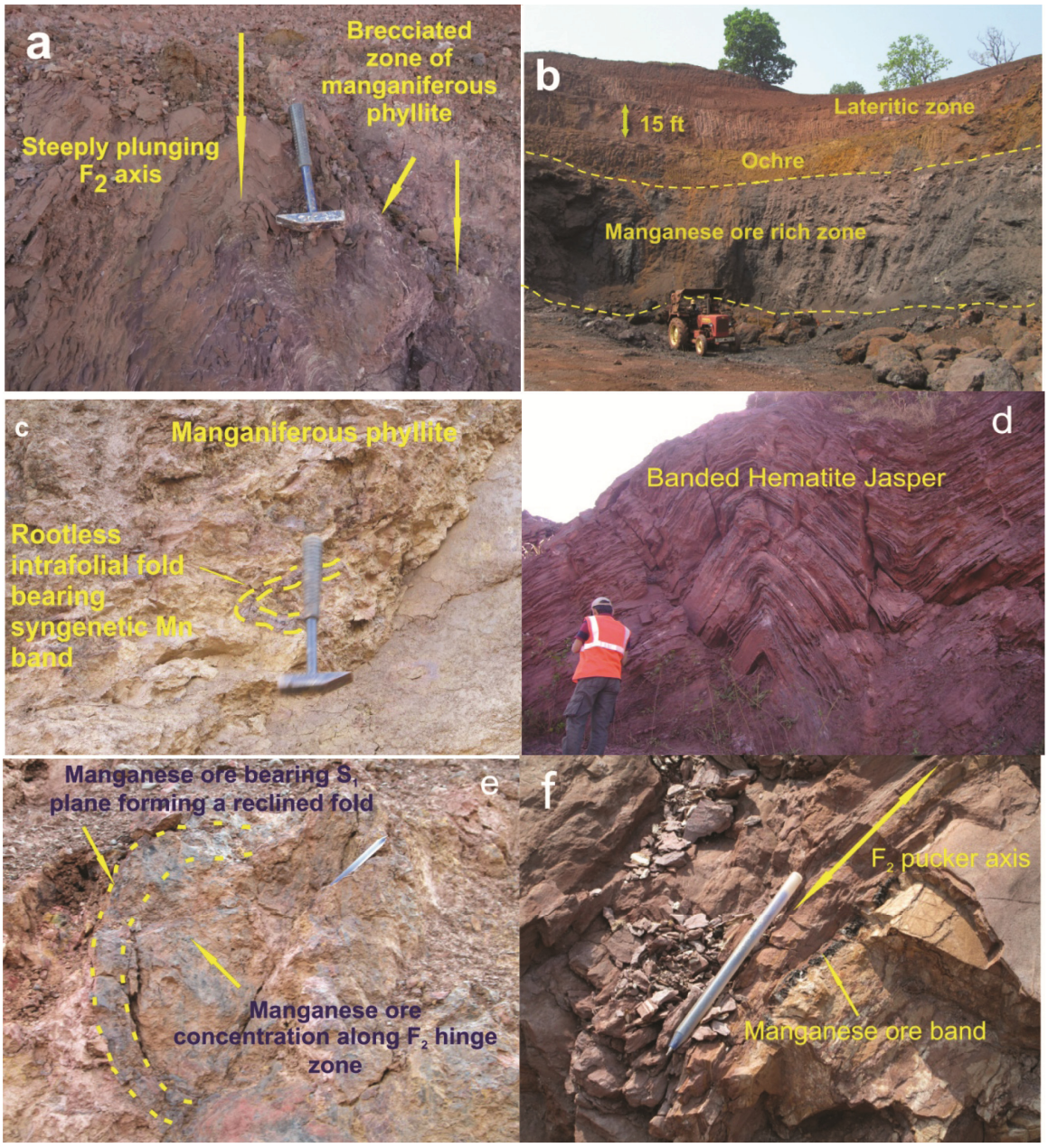
a
Brecciated zone of manganiferous phyllite
Steeply plunging F_2 axis
b
15 ft
Lateritic zone
Ochre
Manganese ore rich zone
c
Manganiferous phyllite
Rootless intrafolial fold bearing syngenetic Mn band
d
Banded Hematite Jasper
Manganese ore bearing S_1 plane forming a reclined fold
e
Manganese ore concentration along F_2 hinge zone
f
F_2 pucker axis
Manganese ore band

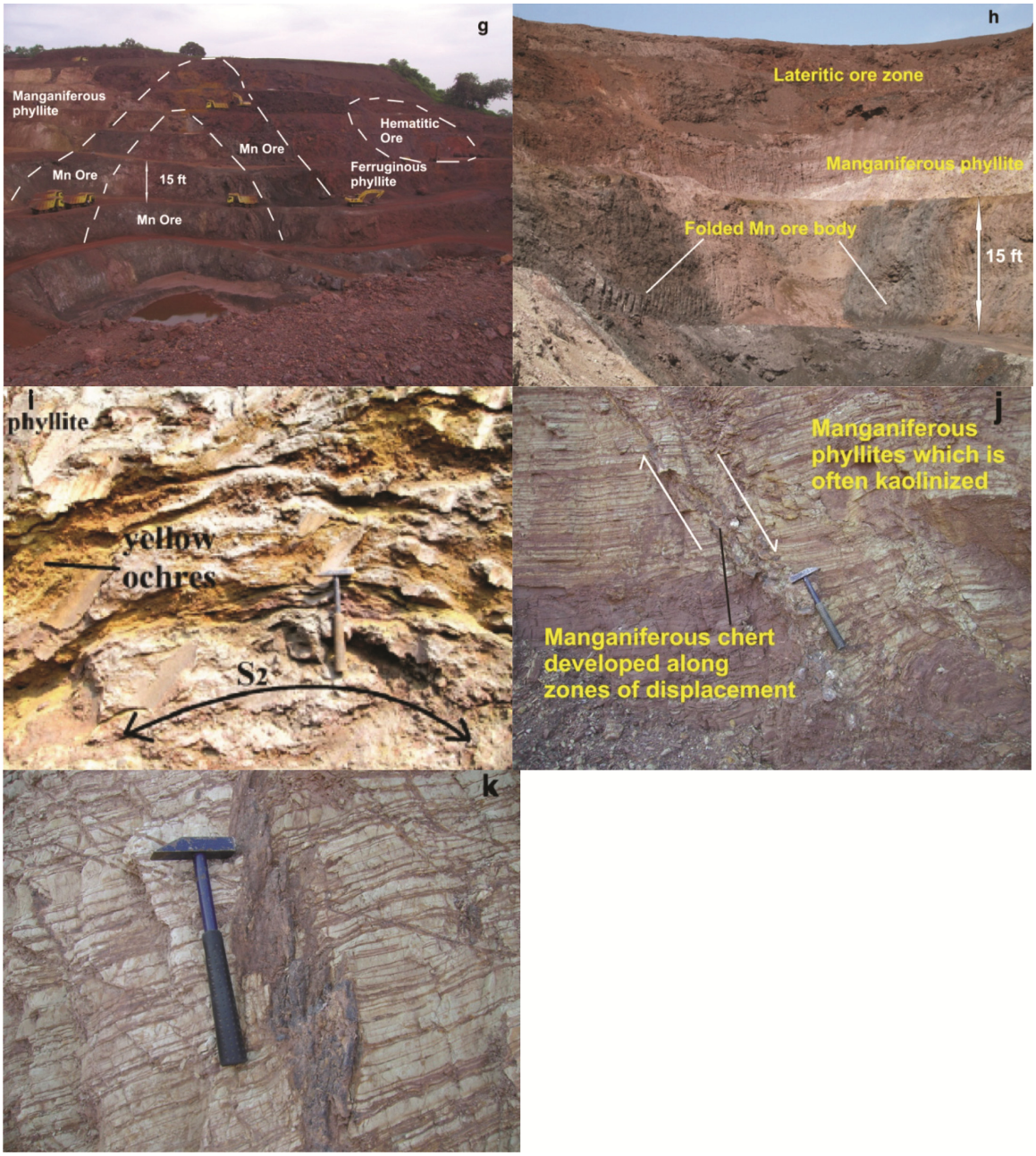

Published by SCHOLINK INC.

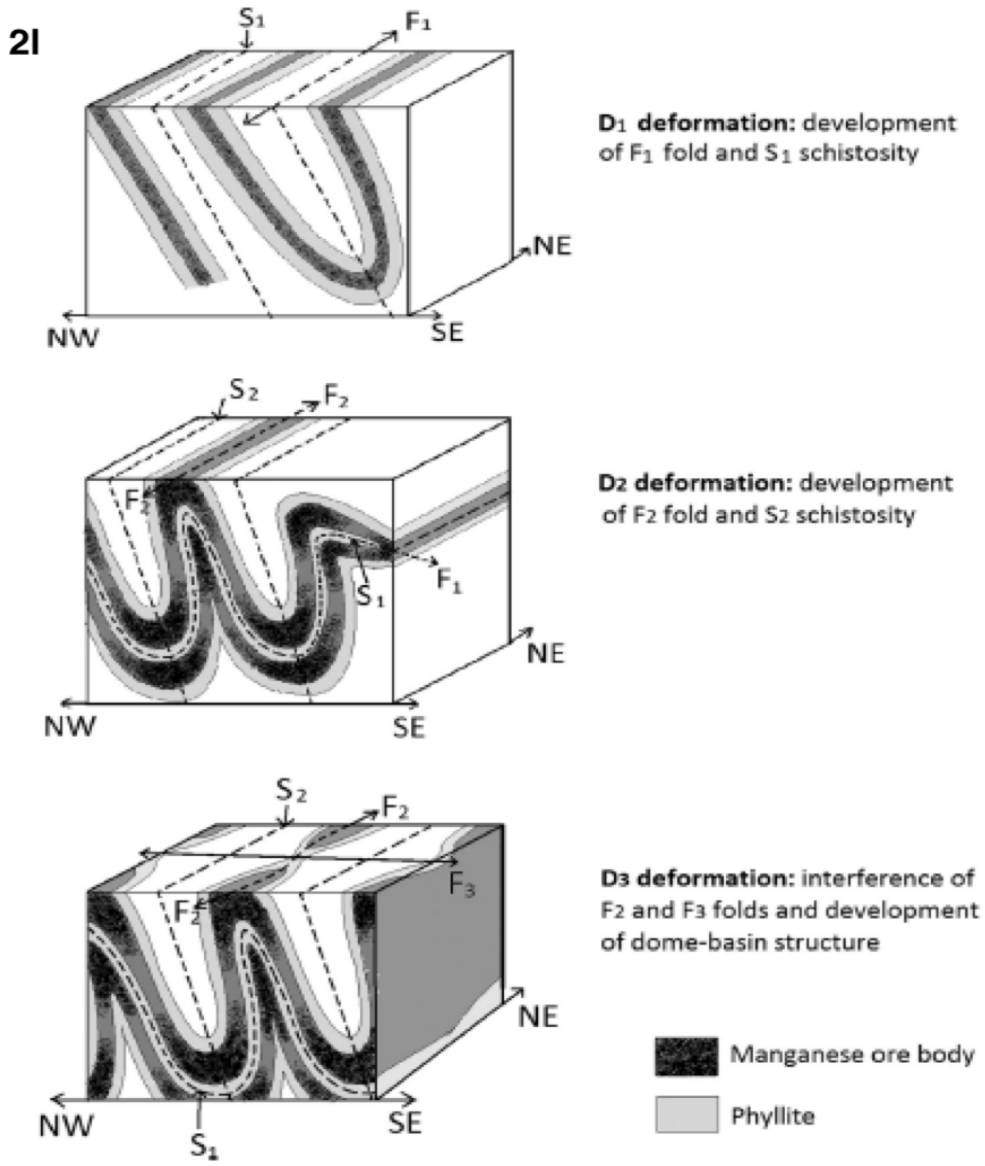

Figure 2. a) Compositionally banded manganiferous phyllite shows brecciated character. b) Mn ore body (hosted by phyllite) is exposed in a quarry section. c) Rootless intrafolial fold reveals strong deformational events. d) Banded Hematite Jasper (BHJ) exhibits its upright folded character. e) Concentration of Mn ore along the F_2 hinge area of a reclined fold. f) Thin manganese ore band follows the S_2 axial plane. g) Quarry section shows folded lithologic units of manganiferous phyllite, Mn ore, ferruginous phyllite and hematitic ore. h) Folded Mn-ore body (hosted by phyllite) is exposed in a quarry section perpendicular to the F_2 axis. Thickness and Mn-ore concentration are maximum at the hinge. i) Open type F_3 folds in Mn ore bodies. Patches of Kaolinite and ochres of variegated colours are also present. j) Normal fault in finely laminated manganiferous phyllite. Manganiferous chert formed along the fault surface. k) Manganiferous chert (black) is infilling a fault zone in the laminated kaolinized phyllite. l) Schematic diagrams showing effects of successive deformational stages of a manganese-ore band in phyllite.

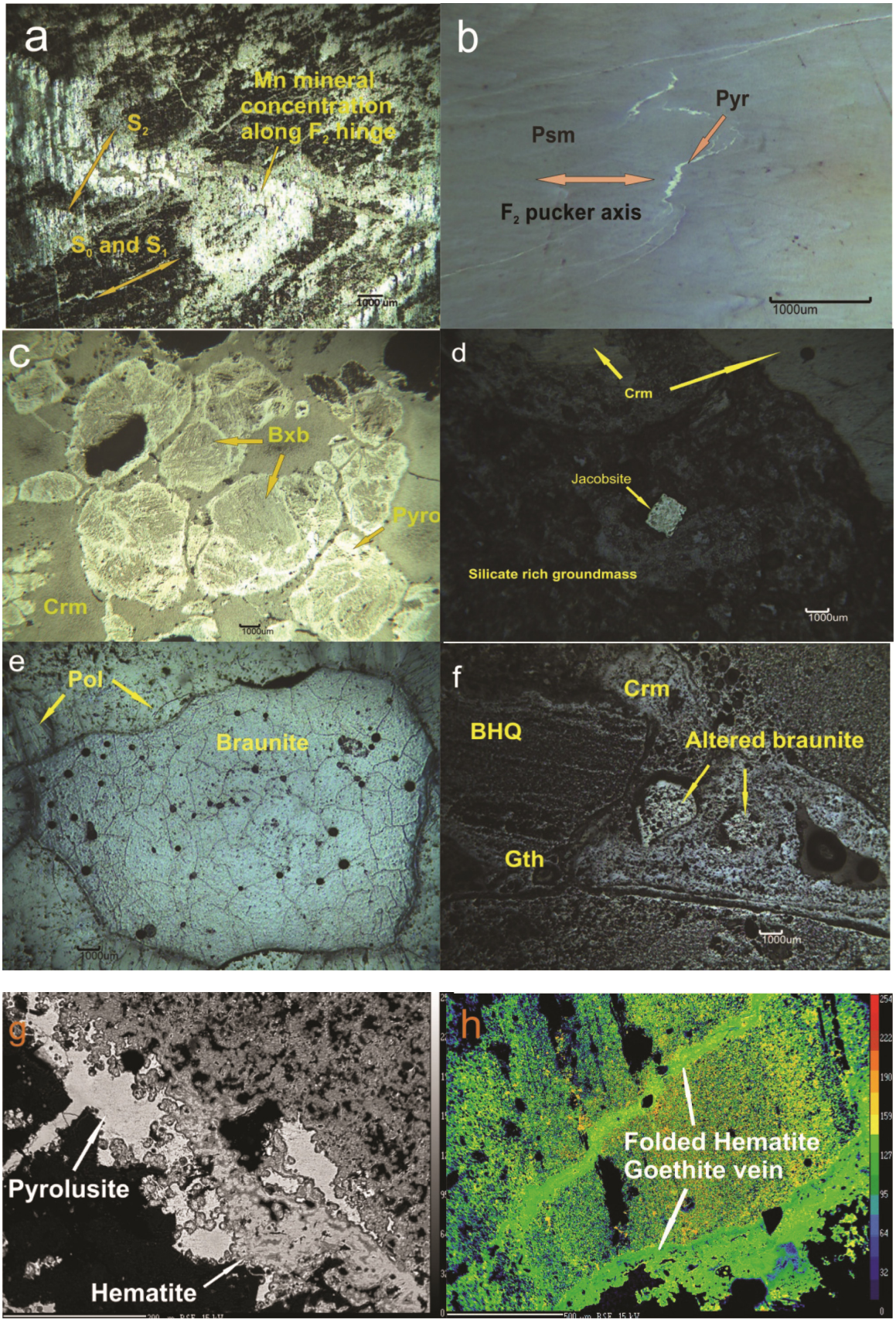
a
Mn mineral concentration along F2 hinge
S2
S0 and S1
1000um
b
Pyr
Psm
F2 pucker axis
1000um
c
Bxb
Pyro
Crm
1000um
d
Crm
Jacobsite
Silicate rich groundmass
1000um
e
Pol
Braunite
1000um
f
Crm
BHQ
Altered braunite
Gth
1000um
g
Pyrolusite
Hematite
h
Folded Hematite
Goethite vein

Figure 3. a) Primary compositional banding (S_0) shows sub-parallel character with first generation cleavage (S_1) whereas S_2 plane showing transgressive relationship with them; Mn ore gets concentrated in the hinge area of F_2 fold. b) Syn-kinematic character to D_2 is exhibited by micro-folded pyrolusite veins. c) Coarse grained bixbyite (Bxb) crystals with matching and resorbed boundaries disseminated in cryptomelane-rich groundmass where pyrolusite and cryptomelane both replacing bixbyite crystals d) Idioblastic jacobsite grain is disseminated within silicate rich groundmass. e) Braunite crystal of earlier generation is being replaced by polianite crystals of later generation. f) Colloform banding of cryptomelane and goethite of later generation at the interstitial spaces of fragmented earlier BHQ and also enclosing altered braunite crystals of earlier generation. g) Pyrolusite and Hematite are closely associated at the contact of silicate and iron rich matrix. h) Hematite-goethite veins are present within the hematite-goethite matrix.

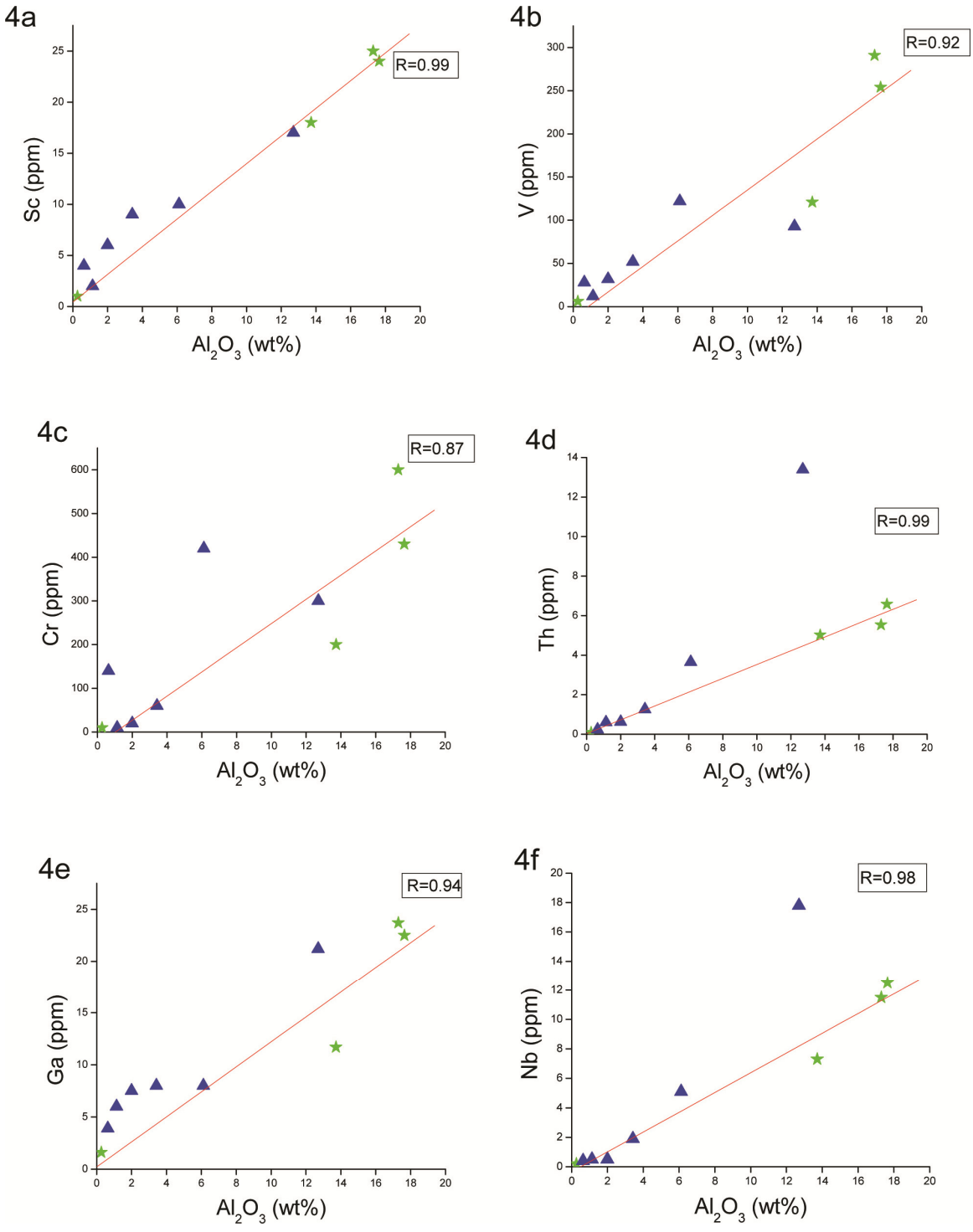

Figure 4. Correlation of Trace Elements Sc, V, Cr, Th, Ga, Nb with Al_2O_3 in Mn-Ores and Host Rocks of Joda Area (Blue Triangles Indicate Ores and Green Stars Indicate Associated Host Rocks)

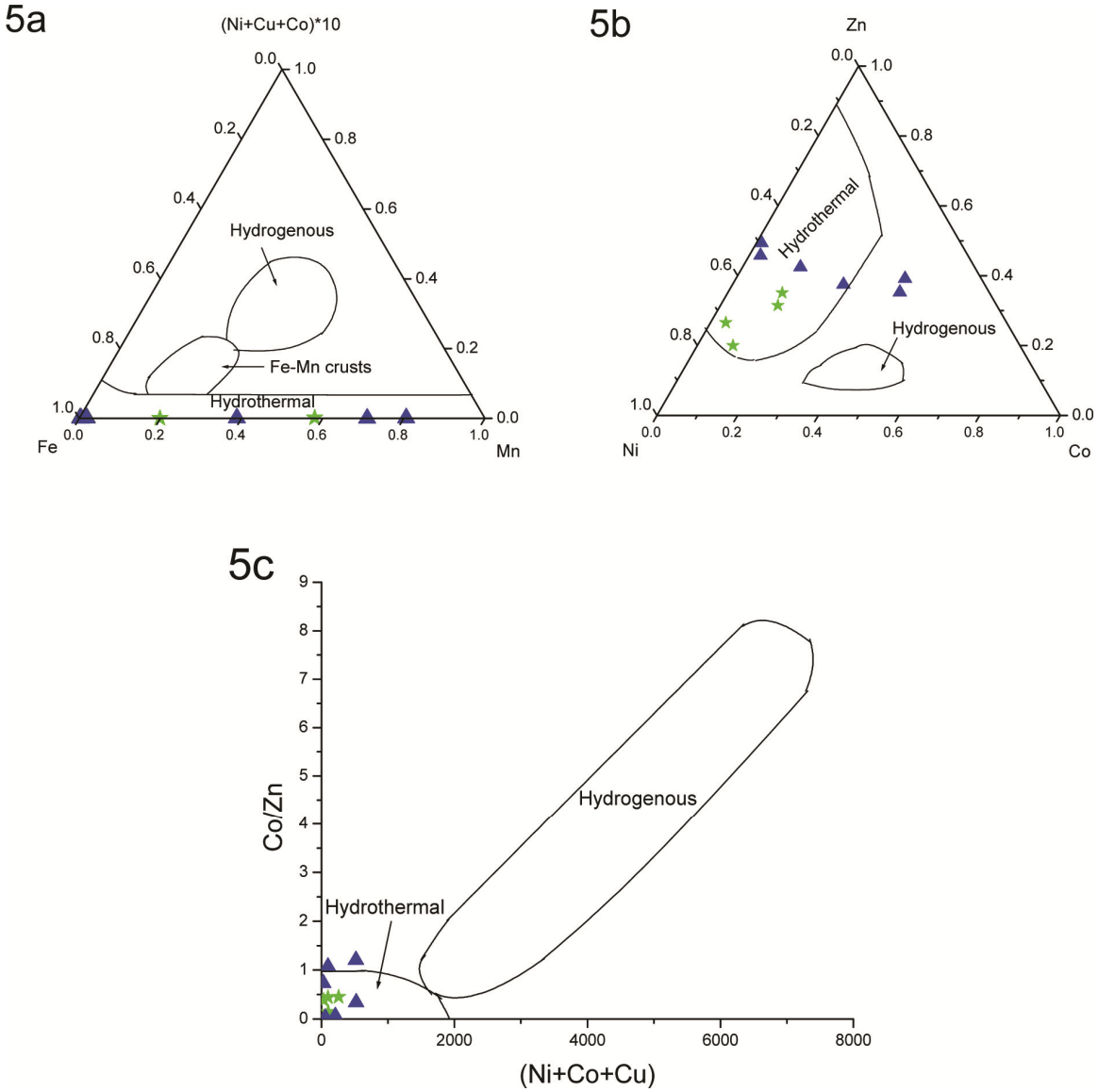

Figure 5. Geochemical Plots of Mn-Ores and Host Rocks in Joda Area (a: diagram from Bonatti et al., 1972, b: diagram from Choi and Hariya, 1992, c: diagram from Toth, 1980) (Blue triangles indicate ores and green stars indicate associated host rocks)

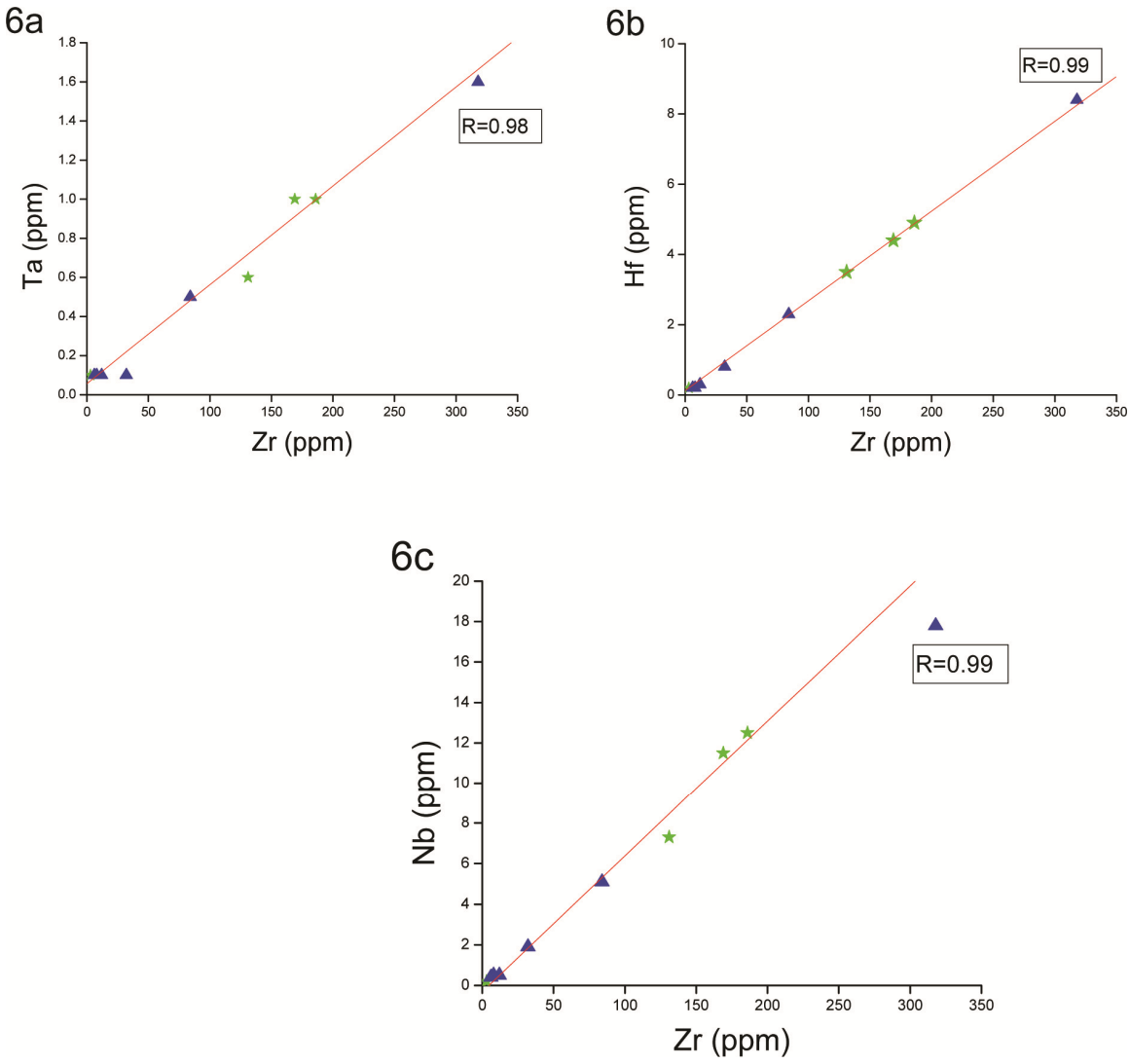

Figure 6. Trace Element Plots for the Immobile Elements Ta, Hf, Nb against Zr in the Mn-Ores of Joda Area (Blue Triangles Indicate Ores and Green Stars Indicate Associated Host Rocks)

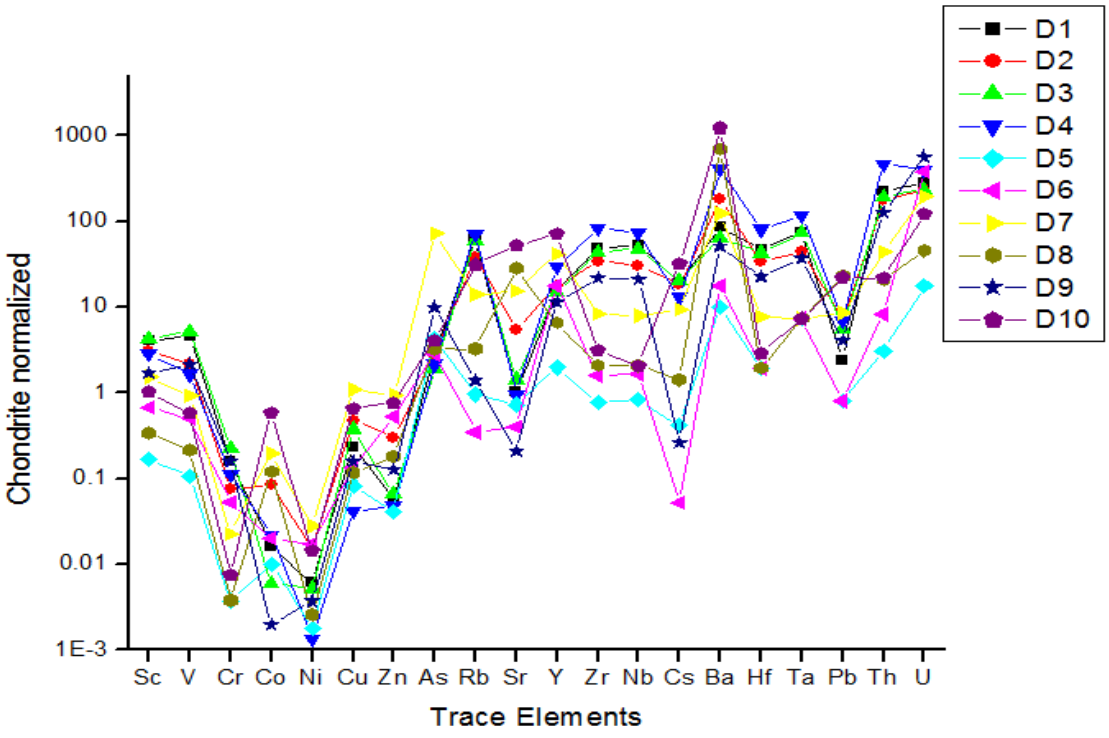

Figure 7. Chondrite Normalized (after McDonough and Sun, 1995) Trace Element Distribution Pattern of Manganese Ores and Associated Rocks of Joda Area

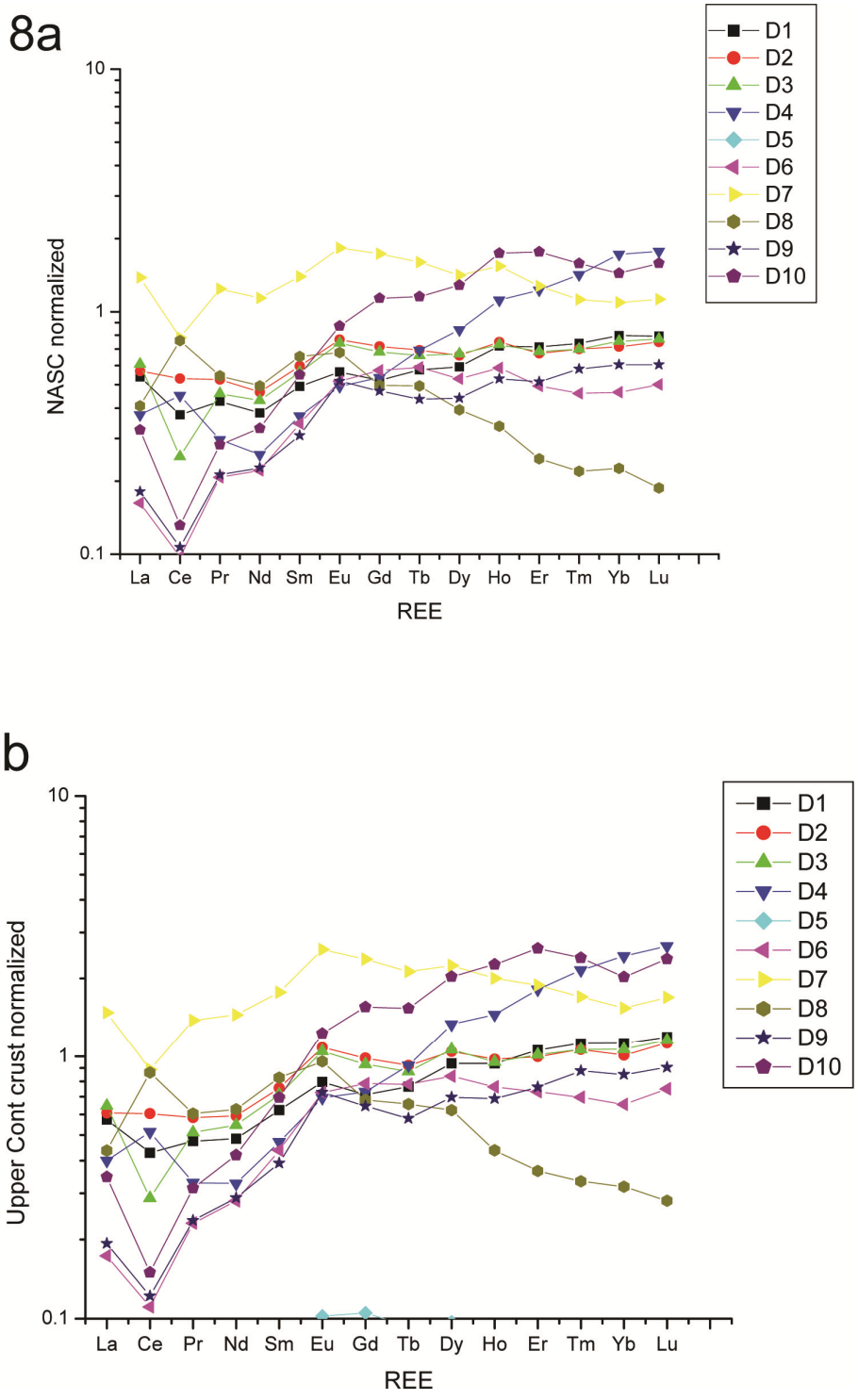

Figure 8. (a) NASC Normalized (after Haskin et al. 1968) and (b) Average Upper Continental Crust Normalized (after Taylor and McLennan, 1981) Rare Earth Abundances of Manganese Ores and Associated Rocks of Joda Area

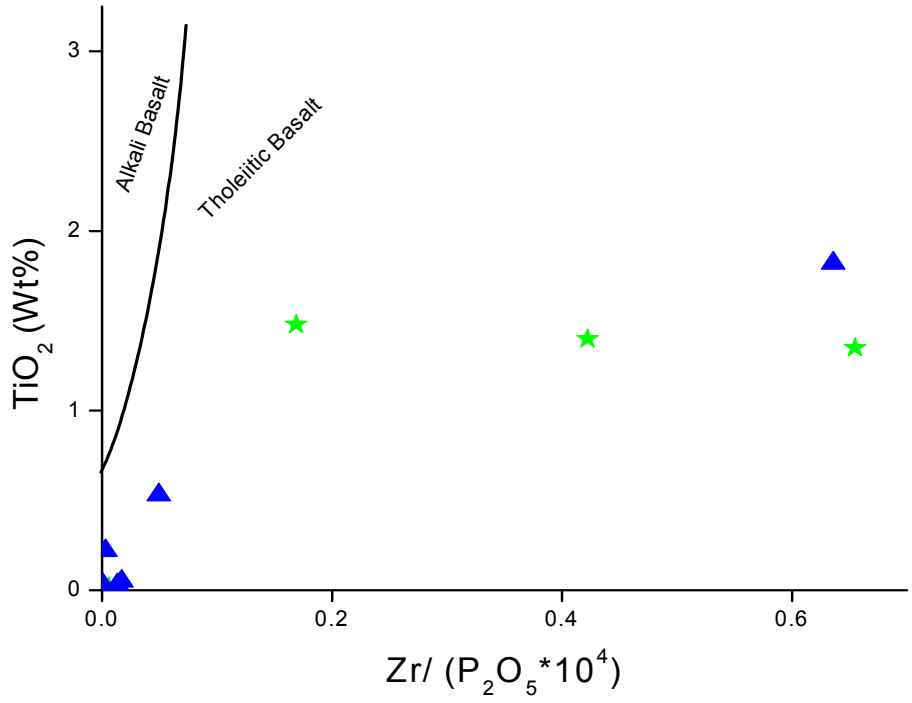

Figure 9. The TiO_2-Zr/(P_2O_5 *10^4) Discrimination Diagram (after Winchester and Floyd, 1976) Manganese Ores and Associated Rocks of Joda Area (Blue Triangles Indicate Ores and Green Stars Indicate Associated Host Rocks)

11. Discussion

The Joda–Noamundi sector in the eastern limb of the Noamundi synclinorium contains significant manganese mineralization. Different tectono-metamorphic events are characterized by distinguished ore mineral assemblages belonging to that particular event.

11.1 Deformation & Metamorphic Events

The earliest deformation and metamorphism event (D_1/M_1) are characterized by the ore mineral assemblage of braunite-bixbyite-jacobsite-hausmannite. The D_2/M_2 event is characterized by the ore mineral assemblage of pyrolusite-psilomelane-hollandite. D_3 stage bears no significant manganese mineralization whereas the post D_3 event is characterized by the hydrothermal pyrolusite-psilomelane-chert association occurring along the faults and shear planes. At the final stage of manganese mineralization, supergene activity/lateritization has formed the ore mineral assemblage of polianite-pyrolusite-psilomelane-manganite-goethite precipitated from colloidal solution replacing earlier manganese minerals. The presence of jacobsite-hausmannite assemblage along with triple junction shown by recrystallized bixbyite grains infer that the peak metamorphic condition during D_1/M_1 attained upper green schist to amphibolite facies, if not higher.

11.2 Major & Trace Element Analysis

Strong positive correlations between Sc and Al_2O_3 (**Figure 4a**), V and Al_2O_3 (**Figure 4b**), Cr and Al_2O_3 (**Figure 4c**), Th and Al_2O_3 (**Figure 4d**), Ga and Al_2O_3 (**Figure 4e**), Nb and Al_2O_3 (**Figure 4f**) indicate their clastic/detrital origin along with Al_2O_3. The relative enrichment of Sc, V, Cr in comparison with average Zr & Th contents indicates the source of clastic materials to be of basic magmatic affinity. On the other hand, Co, Ni, Cu, Zn do not show any appreciable variation with SiO_2 and Al_2O_3 contents of ores and associated rocks signifying that these elements are not directly linked to terrigenous clastic inputs. On ternary diagrams like Fe-Mn-10 (Ni+Co+Cu) (**Figure 5a**) (after Bonatti et al., 1972) and Zn-Ni-Co (**Figure 5b**) (after Choi & Hariya, 1992) and binary diagram Co/Zn versus Co+Ni+Cu (**Figure 5c**) (after Toth, 1980) and the geochemical data of the ores and host rocks plot in the field of hydrothermal part which depicts a significant role of hydrothermal activities for the enrichment of these highly compatible elements in ore formation process. In the case of chemically incompatible elements, the correlation coefficients for regression lines that pass through the bulk composition and origin can be used to select the most immobile element pair (MacLean & Kranidiotis, 1987). High field strength elements like Nb, Ta, Zr, and Hf, which are widely considered to be immobile, correlate highly with each other in manganese ores of the Joda area. Sedimentary environment and alteration can shift the immobile element concentrations but have little effect on inter-element ratios, which are controlled largely by the source of detritus in the rocks. Within the analytical errors, the chemically incompatible elements Nb, Ta, Hf against Zr plot on regression lines through the origin (**Figure 6 a, b, c**). This means that these elements are geochemically coherent and remain immobile during the ore-forming secondary processes. Pb is assumed to be derived from cryptomelane. Both Ba and Pb do not vary systematically with Al_2O_3 and SiO_2 contents inferring their source to be hydrothermal activities at later stages. Samples of Algoma-type BIF of early Archean age (3.8Ga) from Isua, west Greenland, have Ni values as high as~58ppm (Dymek & Klein, 1988). High abundances of Ni and Cr are also reported from several Archean clastic sedimentary rocks, and are generally explained by the presence of an ultramafic source (e.g., McLennan et al., 1983; Fedo et al., 1996). In the Joda area, average Ni and Cr contents are 100.5 ppm & 219 ppm respectively. This is more akin to the Algoma type character. The relative enrichment of Ti, Zr, Sc in comparison with Th possibly infers a recycling product of earlier volcanogenic metabasic rocks.

11.3 REE Analysis

Manganese ores and associated host phyllites comprise a low overall abundance of LREEs and a flat pattern of HREEs. The lack of marked differentiation between LREE and HREE hints for a basic affinity as mafic or ultramafic end-members are characterized by small degrees of light-heavy REE fractionation. It is observed that there is a small positive Eu anomaly (1.16) and negative Ce anomaly (0.88). Attenuated Eu anomalies account for a more dominating mafic source. Manganese ores of the present area show HREE enrichment, negative Ce anomaly and positive Eu anomaly which are similar to modern ferromanganese sediments near mid-oceanic ridges (Barrett & Jarvis, 1988). In oxic

seawater Ce is removed as CeO_2 or Ce $(OH)_4$ by oxidation reaction. Modern seawater has LREE depletion and negative Ce anomaly (Douville et al., 1999). A positive Eu anomaly is also a typical characteristic of modern manganese hydrothermal deposits in the ocean (Hodkinson et al., 1994). As with the increase of terrigenous components the Ce/La ratio increases, the average value of Ce/La ratio (1.79) in the manganese ores indicates inclusion of volcaniclastic components, suggesting that the REE pattern and the Eu anomalies of the manganese-iron ores in the area are influenced by the mixing of Mn rich sea water and volcaniclastics (Mishra et al., 2007). The process of lateritization can also promote the loss of REE to some extent (Moriyama et al., 2008). The REE patterns shown by the ores and associated rocks represent the end product of a complex series of events that record the properties of the Mn rich solutions subsequently precipitated with volcaniclastic sediments. The TiO_2-Zr/(P_2O_5 *10^4) discrimination diagram reveals the tholeiitic character of the basic rocks which acted as the major source for derivation of the ore-forming elements. Alkali basalts have higher P_2O_5 than tholeiitic basalts for a given Zr content. Thus, it can be postulated that the ultimate origin of the ore and associated host rocks is clearly linked to magma of basic composition with prevailing tholeiitic character.

11.4 Basinal Set-Up for Ore Generation

Roy (1968) proposed the Mn-ores to be of lateritoid type only. Banerji (1977) stratigraphically characterized iron-manganese mineralization in the Jamda-Koira belt as the Noamundi Group of much younger age (c. 1500-1100 Ma) with the following sequence (ascending order): lower shale (tuffaceous shale-phyllite), banded hematite jasper, upper shale (manganiferous shale, tuff and chert), basic intrusion, granitic activity. Sarkar and Saha (1962, 1977) described manganese ore bodies intimately associated with unmetamorphosed shales (occasionally tuffaceous) and chert of the Archean IOG. Banerji (2002) considered a major part of the materials of the IOG rocks was deposited in the miogeosyncline derived from the offshore zone of fracture and volcanism. Evidence of earlier crust is also recorded in detrital zircons from supracrustal rocks of these Archaean Cratons, e.g., ~3.62 Ga from Singhbhum Craton (Goswami et al., 1995; Misra et al., 1999). According to Dunn (1940), Dunn and Dey (1942) and Sarkar and Saha (1977) all the iron formations of Bihar and Orissa belong to one group. Iyengar and Murthy (1982), Banerjee (1982) and Acharya (1984) advocated that the BIFs belong to different age groups. However, the available two age data reported by Mukhopadhyay et al. (2008a) from the dacitic lava from the southern IOG of Daitari area (3506.8±2.3 Ma precision U-Pb SHRIMP zircon age) and Basu et al. (2008) from the volcanic rocks of the western IOG in the Noamundi-Koira Valley (3.4 Ga U-Pb zircon age) strongly raises the doubt about the fact that the previously different age-wise classified three IOG belts surrounding SBG, belong to one stratigraphic sequence. It is noteworthy that no Mn-mineralization is evident from the Gorumahisani-Badampahar and Tomka-Daitari iron ore belts. Moreover, Jamda-Koira belt (including Joda) and the Tomka-Daiteri belt comprise only hematitic iron ores, while in the Gorumahisani-Badampahar belt the iron ore is magnetite-rich. So, the same sedimentary environment in these three belts is difficult to establish at the

present stage. Banerji (1974), Mukhopadhyay (1976), Sarkar (1982), Iyenger and Murthy (1982) have opined that Singhbhum granite is the oldest cratonic block on which the IOG rocks were deposited. According to Saha et al. (1988), around 3.2 Ga there was a development of a tensional regime on either side of Singhbhum Granite (3.3 Ga) following which the BIF were deposited in these basins where SBG acts as the basement of IOG rocks. On the other hand, Baidya (2015) suggests 3500-3200 Ma age of the Iron Ore Group when the greenstone belt was formed with concomitant volcanism, sedimentation and ultramafic-mafic magmatism. The oldest granitoid is referred to as the Older Metamorphic Tonalite Gneiss (OMTG, ~3.4 Ga; Saha, 1994; Goswami et al., 1995; Acharyya et al., 2010) that includes enclaves of meta-sediments and meta-volcanics designated as the Older Metamorphic Group (OMG). Sm-Nd isotopic data from the present work indicates the possible maximum age of the rocks (BIF) in Joda area is 3.46 Ga definitely older than the SBG-type A (c. 3.3 Ga) which acts as the basement of IOG rocks. Supergene alteration and hydrothermal activity at later stages may have been attributed for relatively younger age (2.79 Ga) of banded cherty phyllite. The limited age data of the present study possibly infers that manganese ores and associated rocks are likely to be recycled from still earlier greenstone belts.

12. Conclusion

In addition to megascopic and petrographic analyses, the major, trace and rare earth element geochemistry of the manganese ore and associated phyllitic host rocks of the present area confirm the chemistry of the samples as well as the composition of the source material indicative towards a parent magma of basic affinity. The presence of high temperature mineral assemblages (Jacobsite-hausmannite) in pyrolusite-cryptomelane rich groundmass indicates an earlier high-grade peak metamorphic condition. Manganese, iron and some silica were deposited initially as chemical precipitates in the basin. Major oxides Al_2O_3, SiO_2, K_2O, MgO, Na_2O and TiO_2 appear to be contributed from volcaniclastics and terrigenous detritus. Trace elements appear to be controlled by adsorption on the precipitating Mn and Fe oxides or hydroxides. The manganese ore bearing BIF deposits in a greenstone belt with evidence of volcaniclastic association postulate that BIF hosted manganese-iron ores in and around Joda are akin to Algoma character rather than Lake Superior type. REE distribution pattern, positive Eu anomaly, negative Ce anomaly, Ce/La ratio all indicating a mixing of basic volcaniclastic material with the chemically precipitated ores. Hence, it can be concluded that a basic magma generated in an extensional tectonic set up in Archean time acted as the initial source of present-day ore and associated host rocks of Joda area. These rocks were later subjected to several stages of deformation and metamorphism with subsequent hydrothermal activities and supergene alteration/lateritization leading to further recycling and enrichment of manganese in younger ore formation.

Acknowledgements

The authors acknowledge sincere cooperation and logistic support of M/S Tata Steel Ltd. during fieldwork particularly Mr. Tarun Chakraborty, Mr. Manikant, Mr. Mithun and the present Head of the Natural Resourses Manganese Division, Joda, Odisha. Sm-Nd isotopic studies are done in the Australian laboratory Services, Queensland. EPM analytical studies are done in the Central Petrological Laboratory, Geological Survey of India, Kolkata. Sincere thanks are also due to Ms. Riya Mondal and Mr. Rupam Ghosh of the Dept. of Geological Sciences, Jadavpur University for constructive suggestion and discussion.

References

Acharya, S. (1984). Stratigraphic and structural evolution of the rocks of the iron ore basins in Singhbhum-Orissa iron ore province, India. 'Crustal Evolution of the Indian Shield and its Bearing on Metallogeny'. In *Seminar Volume* (pp. 19-28). Indian Society of Earth Sciences, Calcutta.

Acharyya, S. K., Gupta, A., & Oriashi, Y. (2010). New U-Pb zircon ages from Paleo-Mesoarchean TTG gneisses of the Singhbhum craton, Eastern India. *Geochemical Journal*, *44*, 81-88. https://doi.org/10.2343/geochemj.1.0046

Anhaeusser, C. R., & Wilson, J. F. (1981). Southern Africa: The granitic-gneiss greenstone shield. In D. R. Hunter (Ed.), *Precambrian of the Southern Hemisphere* (pp. 423-499). Elsevier, Amsterdam. https://doi.org/10.1016/S0166-2635(08)70202-0

Baidya, T. K. (2015). Archean Metallogeny and Crustal Evolution in the East Indian Shield. *Special Issue: Archean Metallogeny and Crustal Evolution*, *4*, 1-14. https://doi.org/10.11648/j.earth.s.2015040401.11

Banerjee, P. K. (1982). Stratigraphy, petrology and geochemistry of some Precambrian basic volcanic and associated rocks of Singhbhum district, Bihar and Mayurbhanj and Keonjhar districts, Orissa. *Geological Survey of India*, *111*, 1-54.

Banerji, A. K. (1974). On the stratigraphy and tectonic history of the Iron Ore bearing and associated rocks of Singhbhum and adjoining areas of Bihar and Orissa. *Journal of Geological Society, India*, *15*(2), 150-157.

Banerji, A. K. (1977). On the Precambrian banded iron-formations and the manganese ores of the Singhbhum region, Eastern India. *Economic Geology*, *72*(1), 90-98. https://doi.org/10.2113/gsecongeo.72.1.90

Banerji, A. K. (2002). On the Precambrian Banded Iron-Formations and the Manganese ores of the Singhbhum region, Eastern India. *Indian Journal of Geology*, *74*, 1-12.

Barrett, T. J., &Jarvis, I. (1988). Rare-earth element geochemistry of the metalliferous sediments from DSDP Leg 92: The East Pacific Rise Transect. *Chemical Geology*, *67*, 243-259. https://doi.org/10.1016/0009-2541(88)90131-3

Basu, A. R., Bandyopadhyay, P. K., Chakrabarti, R., & Zhou, H. (2008). Large 3.4 Ga Algoma-type BIF in the Eastern Indian craton. *Goldschmidt Conference Abstracts, Chemical Geology*, *72*, A59.

Basu, N. K. (1969). Origin of lateroid manganese deposit of Keonjhar district, Orissa. *Journal of Geology, Mineral & Metallurgical Society, India*, *41*, 183-187.

Bonatti, E., Kraemer, T., & Rydell, H. (1972). Classification and genesis of iron manganese deposits. In D. R. Horn (Ed.), *Ferro-manganese deposits on the ocean floor, Washington, National Science Foundation* (pp. 149-166).

Cameron, E. M., & Garrels, R. M. (1980). Geochemical compositions of some Precambrian shales from the Canadian Shield. *Chemical Geology*, *28*, 181-197. https://doi.org/10.1016/0009-2541(80)90046-7

Chadwick, B., Ramakrishnan, M., & Viswanatha, M. N. (1981a). Structural and metamorphic relations between Sargur and Dharwar supracrustal rocks and Peninsular Gneiss in central Karnataka. *Journal of Geological Society, India*, *22*, 557-569.

Chadwick, B., Ramakrishnan, M., & Viswanatha, M. N. (1981b). The stratigraphy and structure of the Chitradurga region: An illustration of cover-basement interaction in the late Archaean evolution of the Karnataka craton, southern India. *Precambrian Research*, *16*, 31-54. https://doi.org/10.1016/0301-9268(81)90004-8

Chakraborty, K. L., & Majumder, T. (1986). Geological aspects of the banded iron formation of Bihar and Orissa. *Journal of Geological Society, India*, *28*, 109-133.

Choi, J. H., & Hariya, Y. (1992). Geochemistry and depositional environment of manganese oxide deposits in Tokoro belt, northeastern Hokkaido, Japan. *Economic Geology*, *87*(5), 1265-1274. https://doi.org/10.2113/gsecongeo.87.5.1265

Condie, K. C. (1981). *Archean Greenstone Belts*. Elsevier, Amsterdam.

De Wit, M., Hart, R., Stern, C., & Barton, C. M. (1980). Metallogenesis related to seawater interaction with 3.5 b.y. oceanic crust. *Eos*, *61*, 386.

Dimroth, E., Imrch, L., Rocheleau, M., & Goulet, N. (1982). Evolution of the south-central of the Archean Abitibi belt, Quebec. Part I: stratigraphy and paleogeographic model. *Canadian Journal of Earth Sciences*, *19*, 1729-1758. https://doi.org/10.1139/e82-154

Douville, E., Bienvenu, P., Charlou, J. L., Donval, J. P., Fouquet, Y., Appriou, P., & Gamo, T. (1999). Yttrium and rare earth elements in fluids from various deep-sea hydrothermal systems. *Geochimica Cosmochimica Acta*, *63*, 627-643. https://doi.org/10.1016/S0016-7037(99)00024-1

Dunn, J. A. (1940). The stratigraphy of south Singhbhum. *Geological Survey of India, Memoir*, *63*, 303-309.

Dunn, J. A., & Dey, A. K. (1942). The geology and petrology of eastern Singhbhum and surrounding areas. *Memoir Geological Survey of India*, *69*, 281-450.

Dymek, R. F., & Klein, C. (1988). Chemistry, petrology and origin of banded iron formation lithologies from the 3800 Ma Isua supracrustal province, West Greenland. *Precambrian Research*, *39*, 247-302. https://doi.org/10.1016/0301-9268(88)90022-8

Engineer, B. B. (1956). Geology and Economic Aspects of the Manganese Ore Deposits of Jamda-Koira Valley, Keonjhar, Bonai, Orissa, India. *20th International Geological Congress, Symposium on Manganese*, *4*, 26-40.

Fedo, C. M., & Eriksson, K. A. (1996). Stratigraphic framework of the 3.0 Ga Buhwa greenstone belt: a unique stable-shelf succession in the Zimbabwe Archean craton. *Precambrian Research*, *77*, 161-178. https://doi.org/10.1016/0301-9268(95)00053-4

Ghosh, R., Chakraborty, D., Halder, M., & Baidya, T. K. (2015). Manganese mineralization in Archean greenstone belt, Joda-Noamundi sector, Noamundi basin, East Indian Shield. *Ore Geology Reviews*, *70*, 96-109. https://doi.org/10.1016/j.oregeorev.2015.04.007

Goldstein, S. L., O'nions, R. K., & Hamilton, P. J. (1984). A Sm-Nd isotopic study of atmospheric dusts and particulates from major river systems. *Earth and Planetary Science Letters*, *70*, 221-236. https://doi.org/10.1016/0012-821X(84)90007-4

Goodwin, A. M. (1973). Archean iron-formation and tectonic basins of the Canadian Shield. *Economic Geology*, *68*, 915-933. https://doi.org/10.2113/gsecongeo.68.7.915

Goswami, J. N., Misra, S., Wiedenback, M., Ray, S. L., & Saha, A. K. (1995). 3.55 Ga old zircon from Singhbhum–Orissa Iron Ore craton, eastern India. *Current Science*, *69*, 1008-1011.

Grommet, L. P., Dymek, R. F., Haskin, L. A., & Korotev, R. L. (1984). The "North American shale composite": Its compilation, major and trace element characteristics. *Geochimica Cosmochimica Acta*, *48*, 2469-2482. https://doi.org/10.1016/0016-7037(84)90298-9

Gross, G. A. (1986). The metallogenetic significance of iron-formation and related stratified rocks. *Journal of Geological Society, India*, *28*, 92-108.

Hallberg, J. A., & Glikson, A. Y. (1981). Archean granite-greenstone terrains of W. Australia. In D. R. Hunter (Ed.), *Precambrian of the Southern Hemisphere* (pp. 33-103). Elsevier, Amsterdam. https://doi.org/10.1016/S0166-2635(08)70196-8

Haskin, L. A., Haskin, M. A., Frey, F. A., & Wildman, T. R. (1968). Relative and absolute terrestrial abundances of the rare earths, In L. H. Ahrens (Ed.), *Origin and distribution of the elements* (Vol. 1, pp. 889-911). Pergamon, Oxford. https://doi.org/10.1016/B978-0-08-012835-1.50074-X

Hodkinson, R. A., Stoffers, P., Scholten, J., Cronan, D. S., Jeschke, G., & Rogers, T. D. S. (1994). Geochemistry of hydrothermal manganese deposits from the Pitcairn Island hotspot, southeastern Pacific. *Geochimica Cosmochimica Acta*, *58*, 5011-5029. https://doi.org/10.1016/0016-7037(94)90228-3

Iyenger, S. V. P., & Murthy, Y. G. K. (1982). The evolution of the Archaean Proterozoic crust in parts of Bihar and Orissa, eastern India. *Geological Survey of India Records*, *112*, 1-5.

Jones, H. C. (1934). The iron ore deposits of Bihar and Orissa. *Memoir Geological Survey of India*, *63*(2), 167-302.

Machado, N., & Carnerio, M. (1992). U-Pb evidence of Late Archean tectono-thermal activity in the southern Sao Francisco Shield, Brazil. *Canadian Journal of Earth Sciences*, *29*, 2341-2346. https://doi.org/10.1139/e92-182

MacLean, W. H., & Kranidiotis, P. (1987). Immobile elements as monitors of mass transfer in hydrothermal alteration; Phelps Dodge massive sulfide deposit, Matagami, Quebec. *Society of Economic Geology*, *82*(4). https://doi.org/10.2113/gsecongeo.82.4.951

Martin, H., Peucat, J. J., Sabate, P., & Cunha, J. C. (1997). Crustal evolution in the Early Archean of South America: Example of the Sete Voltas Massif, Bahia State, Brazil. *Precambrian Research*, *82*, 35-62. https://doi.org/10.1016/S0301-9268(96)00054-X

McDonough, W. F., & Sun, S. S. (1995). The Composition of the Earth. *Chemical Geology*, *120*, 223-253. https://doi.org/10.1016/0009-2541(94)00140-4

McLennan, S. M., & Taylor, S. R. (1983). Geochemical evolution of Archean Shales from South Africa. 1. The Swaziland and Pongola Supergroup. *Precambrian Research*, *22*, 93-124. https://doi.org/10.1016/0301-9268(83)90060-8

McLennan, S. M., Taylor, S. R., & Eriksson, K. A. (1983). Geochemistry of Archean shales from Pilbara Supergroup, Western Australia. *Geochimica Cosmochimica Acta*, *47*, 1211-1222. https://doi.org/10.1016/0016-7037(83)90063-7

Mishra, P. P., Mohapatra, B. K., & Singh, P. P. (2007). Contrasting REE signatures on manganese ores of Iron Ore Group in North Orissa, India. *Journal of Rare Earths*, *25*, 749-758. https://doi.org/10.1016/S1002-0721(08)60020-4

Mishra, P., Mohapatra, B. K., & Singh, P. P. (2006). Mode of occurrence and characteristics of Mn-ore bodies in Iron Ore Group of rocks, North Orissa, India and its significance inresource evaluation. *Resource Geology*, *56*, 55-64. https://doi.org/10.1111/j.1751-3928.2006.tb00268.x

Misra, S., Deomurari, M. P., Wiedenbeck, M., Goswami, N. J., Ray, S., & Saha, A. K. (1999). 207Pb/206Pb zircon ages and the evolution of the Singhbhum craton, eastern India: an ion microprobe study. *Precambrian Research*, *93*, 139-151. https://doi.org/10.1016/S0301-9268(98)00085-0

Mohapatra, B. K., Paul, D., & Sahoo, R. K. (1996). REE distribution in ferromanganese oxide ores from Iron Ore Group, Western Koira Valley, Orissa, India. *Journal of Mineralogy, Petrology and Economic Geology (Japan)*, *91*, 266. https://doi.org/10.2465/ganko.91.266

Moriyama, T., Panigrahi, M. K., Pandit, D., & Watanabe, Y. (2008). Rare Earth Element Enrichment in Late Archean Manganese Deposits from the Iron Ore Group, East India. *Resource Geology*, *58*, 402-413. https://doi.org/10.1111/j.1751-3928.2008.00072.x

Mukhopadhyay, D. (1976). Precambrian stratigraphy of Singhbhum: The problems and a prospect. *Indian Journal of Earth Science*, *3*, 208-219.

Mukhopadhyay, J., Beukes, N. J., Armstrong, R. A., Zimmermann, U., Ghosh, G., & Medda, R. A. (2008a). Dating the Oldest Greenstone in India: A 3.51-Ga Precise U-Pb SHRIMP Zircon Age for Dacitic Lava of the Southern Iron Ore Group, Singhbhum craton. *Journal of Geology*, *116*, 449-461. https://doi.org/10.1086/590133

Murthy, V. N., & Ghosh, B. K. (1971). Manganese ore deposit of the Bonai-Keonjhar belt, Orissa, Indian Minerals. *Geological Survey of India Publication*, *25*(3), 201.

Myers, J. S., & Kröner, A. (1994). *Archean Tectonics: Continental Deformation* (P. L. Hancock, Ed., pp. 355-369). Pergamon Press, Oxford.

Prasad, R., & Murty, Y. G. K. (1956). Manganese Ore Deposits of Orissa and Bihar, India. *20th International Geological Congress, Symposium on Manganese*, *4*, 115-131.

Ramakrishnan, M., Viswanatha, M. N., & Swami, N. J. (1976). Basement-cover relationships of Peninsular gneiss with high grade schists and greenstone belts of southern Karnataka. *Journal of Geological Society of India*, *17*, 97-111.

Roy, S. (1968). Mineralogy of the different types of manganese deposits. *Economic Geology*, *63*, 760-788. https://doi.org/10.2113/gsecongeo.63.7.760

Roy, S. (1978). Manganese Ore Deposit of India. In I. M. Varentsov (Ed.), *Geology and Geochemistry of Manganese* (Vol. 2). Peoples Publishing House of the Hungarian Academy of Sciences

Roy, S. (1981). *Manganese Deposits*. Academic Press, London.

Saha, A. K., Ray, S. L., & Sarkar, S. N. (1988). Early history of the Earth: Evidence from the Eastern Indian shield. *Memoir Geological Society of India*, *8*, 13-37.

Sarkar, S. N., & Saha, A. K. (1962). A revision of Precambrian stratigraphy and tectonics of Singhbhum and adjacent regions. *Quaternary Journal of the Geological Mining Metallurgical Society of India*, *34*, 97-136.

Sarkar, S. N., & Saha, A. K. (1977). The present state of Precambrian stratigraphy, tectonics and geochronology of Singhbhum–Keonjhar–Mayurbhanj region, Eastern India. *Indian Journal of Earth Science*, 37-66.

Schidlowski, M. (1988). A 3800-million-year isotopic record of life from carbon in sedimentary rocks. *Nature*, *333*, 313-318. https://doi.org/10.1038/333313a0

Sen, B. (1951). Manganese ores of Keonjhar. *Transactions of the Mining, Geological and Metallurgical Institute of India*, *47*, 85-111.

Spencer, E. (1948). The manganese ore deposits of Jamda-Koira Valley. *Transactions of the Mining, Geological and Metallurgical Institute of India*, *44*.

Subramanyam, M. R., & Murthy, V. N. (1975). Iron formation of Bonai–Keonjhar and the iron ore group of North Orissa. *Journal of Chayantica Geology*, *1*, 77-90.

Taylor, S. R., & McLennan, S. M. (1981). The composition and evolution of the continental crust: Rare earth element evidence from sedimentary rocks. *Philosophical Transactions of the Royal Society of London*, *301*, 381-399. https://doi.org/10.1098/rsta.1981.0119

Teixeira, W., Carneiro, M. A., Noce, C. M., Machado, N., Sato, K., & Taylor, P. N. (1996). Pb, Sr and Nd isotope constraints on the Archean evolution of gneissic-granitoid complexes in the southern Sao Francisco craton, Brazil. *Precambrian Research*, *78*, 151-164. https://doi.org/10.1016/0301-9268(95)00075-5

Toth, J. R. (1980). Deposition of submarine crusts rich in manganese and iron. *Geological Society of America Bulletin*, *91*, 44-54. https://doi.org/10.1130/0016-7606(1980)91<44:DOSCRI>2.0.CO;2

Winchester, J. A., & Floyd, P. A. (1976). Geochemical magma type discrimination; application to altered and metamorphosed basic igneous rocks. *Earth and Planetary Science Letters*, *28*, 459-469. https://doi.org/10.1016/0012-821X(76)90207-7

Windly, B. F. (1982). *The Evolving Continents* (2nd ed., pp. 28-65). John Wiley & Publication.